

## Unsteady Mixed Convection Flow in the Stagnation Region of a Three Dimensional Body Embedded in a Porous Medium

F. S. Ibrahim

Department of Mathematics, Faculty of Science  
Assiut University  
Assiut, Egypt  
fibrahim@aun.edu.eg

**Received:** 12.04.2007    **Revised:** 30.08.2007    **Published online:** 06.03.2008

**Abstract.** An analysis is performed to study the heat transfer characteristic of unsteady mixed convection flow of a viscous fluid in the vicinity of a stagnation point of a general three-dimensional body embedded in a porous media. The velocity in the potential flow is assumed to vary arbitrary with time. The non-Darcy effects including convective, boundary and inertial effects are included in the analysis. Both nodal-point region ( $0 \leq c \leq 1$ ), where  $c = b/a$  is the ratio of the velocity gradients in  $y$  and  $x$  directions in the potential flow and saddle point region ( $-1 \leq c < 0$ ), are considered. The semi-similar solutions of the momentum and energy equations are obtained numerically using finite difference method. Also a self-similar solution is found when the velocity in the potential flow and the wall temperature vary with time in particular manner. Many results are obtained and a representative set is displayed graphically to illustrate the influence of the physical parameters on the surface shear stresses and the surface heat transfer.

**Keywords:** unsteady flow, mixed convection, stagnation-point, self-similar solution, porous media.

### Nomenclature

$a, b$	principal curvatures of the body at the stagnation point
$c$	curvature ratio at the stagnation point
$C_{fx}$	surface skin friction coefficient in the $x$ direction
$C_{fy}$	surface skin friction coefficient in the $y$ direction
$c_p$	specific heat at a constant pressure
$E, E_1$	Eckert numbers
$f$	dimensionless velocity component in the $x$ direction
$g$	acceleration due to gravity
$g(\eta, t^*)$	dimensionless temperature
$Gr_x$	local Grashof number
$k$	thermal conductivity

$K$	permeability
$Nu_x$	local Nusselt number
$Pr$	Prandtl number
$Re_x$	local Reynolds number
$s$	dimensionless velocity component in the $y$ direction
$t$	time
$t^*$	dimensionless transformed independent variable based on time
$T$	temperature
$u, v, w$	velocity components in the $x, y$ and $z$ directions, respectively
$x, y, z$	local orthogonal coordinates with $x$ and $y$ axes along the body surface and $z$ axis normal to the surface

**Greek symbols**

$\alpha$	thermal diffusivity
$\beta$	bulk coefficient of thermal expansion
$\chi$	mixed convection parameter
$\Delta$	second order resistance
$\varepsilon$	porosity
$\phi$	dimensionless velocity component in the $z$ direction
$\eta$	dimensionless transformed independent variable based on $z$
$\gamma$	first order resistance
$\Gamma$	empirical constant
$\lambda$	dimensionless parameter which characterizes the unsteadiness in the flow field
$\mu$	fluid dynamic viscosity
$\nu$	fluid kinematics viscosity
$\rho$	fluid density

**Subscripts**

$i$	initial condition
$w$	wall condition
$\infty$	condition in the ambient fluid

**Superscript**

'	denotes derivative with respect to $\eta$
---	---

## 1 Introduction

Convective heat transfer in fluid-saturated porous media has important applications in both technology and geothermal energy recovery. Most of the recent research on convective flow in porous media has been directed to the problems of steady free and mixed convection flows over heated bodies embedded in fluid-saturated porous media. However, unsteady convective boundary layer flow problems have not, so far, received as much attention. The analysis of many practical fluid mechanics problems depends on understanding the behavior of the unsteady boundary layer. It is of interest in problems

covering dynamic stall of helicopters, rotor blades, and turbo machinery, acoustics, aeronautics and missile aerodynamics. For such wide applications as geothermal serves the design of high temperature insulation and reactors and thin film separation in chemical processes. Perhaps, the first study on unsteady boundary layer flow on flat surfaces in porous media was made by Johnson and Cheng [1] who found similarity solutions for certain variations of the wall temperature. The more common cases, in general, involve transient convection, which is non-similar and hence, more complicated mathematically. The interested reader can find an excellent collection of papers on unsteady convective flow problems over heated bodies embedded in a fluid-saturated porous medium in the review papers by Bradean et al. [2] and in the book by Pop and Ingham [3].

The present paper address the problem of mixed convection flow in the region of a general three-dimensional stagnation point (i.e., nodal or saddle point) of a body embedded in a porous medium in the presence of first and second orders resistances, which to the best of our knowledge have not been investigated yet. Although the problem of mixed convection flow over three-dimensional bodies embedded in porous media has not been studied very much, the corresponding case of clear (non-porous) fluid has been investigated by a number of researchers. The unsteady three-dimensional free convection flow in the stagnation-point region on a general curved isothermal surface placed in an ambient fluid was studied by Hang et al. [4]. Eswara and Nath [5] studied the unsteady laminar incompressible mixed convection boundary layer flow with large injection rates at the stagnation point of a three-dimensional body. Kumari and Nath [6] studied the unsteady flow and heat transfer of a viscous fluid in the stagnation region of a three-dimensional body surrounded by a magnetic field.

Several investigations have been carried out also for the two-dimensional case of free and mixed convection in porous media. Nazar et al. [7] have studied the unsteady mixed convection boundary layer flow near the region of a stagnation point on a vertical surface embedded in a Darcian fluid-saturated porous medium. A detailed theoretical study of unsteady free convection boundary-layer flow near the stagnation point of a two-dimensional cylindrical surface embedded in a fluid-saturated porous medium has been studied by Merkin and Pop [8].

Hassanien et al. [9] have studied recently the unsteady free convection flow in the stagnation-point region of a three-dimensional body embedded in a porous media. More recently, the problem of free convection boundary layer flow near a three-dimensional stagnation point of attachment resulting from a step change in its constant surface temperature has been studied by Shafie et al. [10].

Motivation to study mixed convection in porous media comes from the need to characterize the convective transport processes around deep geological repository for the disposal of high-level nuclear waste, e.g. spent fuel rods from nuclear reactors (see Lai [11]).

The aim of the this analysis is to study the development of mixed convection in the stagnation flow of a three-dimensional body embedded in a porous medium in the presence of first and second orders resistances. The semi-similar solutions of the partial differential equations are obtained by the local non-similarity solutions. Also a self-similar solution is found when the velocity in the potential flow and the wall temperature

vary with time in a particular manner.

## 2 Mathematical analysis

Let us consider the unsteady laminar motion of a viscous incompressible fluid in the neighborhood of the forward stagnation point of a three-dimensional body. The physical model and coordinate system are shown in Fig. 1.

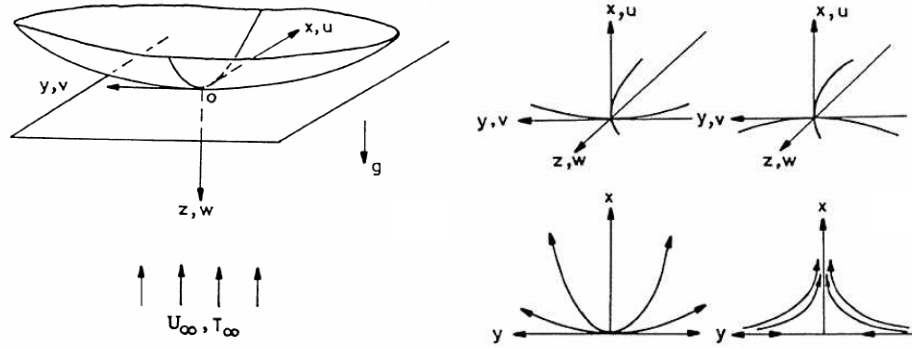


Fig. 1. Schematic representation of coordinates, velocity components and the streamlines in the external stream.

A locally orthogonal set of coordinates  $(x, y, z)$  is chosen with the origin  $o$  at the lowest stagnation point, with  $x$  and  $y$  the coordinates along the body surface and  $z$  the coordinate perpendicular to the body surface at  $o$ . Gravity  $g$  is normal to the surface  $x = 0$  and  $y = 0$  and acts opposite to  $z$  direction. Let  $u, v$  and  $w$  denote the velocity components along  $x, y$  and  $z$  directions, respectively. The parameters  $a$  and  $b$  are the curvatures of the body measured in the planes  $y = 0$  and  $x = 0$ , respectively. The components of buoyancy force in the  $x, y$  and  $z$  directions are  $ax\beta g(T - T_\infty)$ ,  $by\beta g(T - T_\infty)$ , and  $0$  given by Banks [12]. The boundary layer equations of continuity, momentum and energy governing the unsteady flow are given below:

$$\frac{\partial u}{\partial x} + \frac{\partial v}{\partial y} + \frac{\partial w}{\partial z} = 0, \quad (1)$$

$$\frac{Du}{Dt} = -\rho^{-1} \frac{\partial p}{\partial x} + \nu \nabla^2 u + axg\beta(T - T_\infty) - \frac{\nu\varepsilon}{K}u - \frac{\Gamma\varepsilon^2}{K^{12}}u^2, \quad (2)$$

$$\frac{Dv}{Dt} = -\rho^{-1} \frac{\partial p}{\partial y} + \nu \nabla^2 v + byg\beta(T - T_\infty) - \frac{\nu\varepsilon}{K}v - \frac{\Gamma\varepsilon^2}{K^{12}}v^2, \quad (3)$$

$$\frac{Dw}{Dt} = -\rho^{-1} \frac{\partial p}{\partial z} + \nu \nabla^2 w - \frac{\nu\varepsilon}{K}w - \frac{\Gamma\varepsilon^2}{K^{12}}w^2, \quad (4)$$

$$\rho c_p \frac{DT}{Dt} = k \nabla^2 T + \mu \left( \frac{\partial^2 u}{\partial z^2} + \frac{\partial^2 v}{\partial z^2} \right), \quad (5)$$

where

$$\nabla^2 = \frac{\partial^2}{\partial x^2} + \frac{\partial^2}{\partial y^2} + \frac{\partial^2}{\partial z^2}, \quad \frac{D}{Dt} = \frac{\partial}{\partial t} + u \frac{\partial}{\partial x} + v \frac{\partial}{\partial y} + w \frac{\partial}{\partial z}.$$

The initial conditions (i.e., conditions at  $t = 0$ ) are given by

$$u = u_i, \quad v = v_i, \quad w = w_i, \quad p = p_i, \quad T = T_i, \quad \text{at } t = 0. \quad (6)$$

The boundary conditions are

$$\begin{aligned} u = v = w = 0, \quad p = p_0, \quad T = T_w & \quad \text{at } z = 0, \quad x \geq 0, \quad y \geq 0, \\ u \rightarrow U, \quad v \rightarrow V, \quad w \rightarrow W, \quad T \rightarrow T_\infty & \quad \text{as } z \rightarrow \infty, \quad x \geq 0, \quad y \geq 0, \\ u = U, \quad v = V, \quad w = W, \quad T = T_\infty & \quad \text{at } x = 0, \quad y \geq 0, \quad z > 0, \\ u = U, \quad v = V, \quad w = W, \quad T = T_\infty & \quad \text{at } y = 0, \quad x \geq 0, \quad z > 0. \end{aligned} \quad (7)$$

Here  $p$  is the static pressure;  $T$  is the temperature;  $\rho$  and  $\mu$  are the fluid density and the dynamic viscosity, respectively;  $\nu$  is the kinematics viscosity;  $c_p$  is the specific heat at a constant pressure;  $k$  is the thermal conductivity;  $\beta$  is the bulk coefficient of thermal expansion;  $p_0$  is the stagnation pressure;  $U, V$  and  $W$  are the components of velocity in the potential flow;  $\varepsilon, K, \Gamma$  are the porosity, the permeability and empirical constant. The subscripts  $i, w$  and  $\infty$  denote initial condition, condition at the wall and condition at infinity.

### 3 Semi-similar equations

The equations governing the unsteady flow (1)–(5) are partial differential equations with four independent variables ( $t, x, y, z$ ). To reduce these equation to partial differential equations with two independent variables ( $\eta, t^*$ ), the potential velocity components in  $x$  and  $y$  directions are taken in the form (Kumari and Nath [6]):

$$\begin{aligned} U = ax\phi(t^*), \quad V = by\phi(t^*), \\ t^* = at, \quad a = (\partial U / \partial x)_{t^*=0} \quad \text{and} \quad b = (\partial V / \partial y)_{t^*=0}. \end{aligned} \quad (8)$$

Substituting from equation (8) into the equation of continuity (1), we can get the third component of the potential velocity in the form.

$$W = -a(1+c)z\phi(t^*), \quad c = b/a. \quad (9)$$

Using the three-dimensional unsteady Bernoulli equation, the pressure  $p$  is given by

$$\begin{aligned} p_0 - p = \frac{\rho a^2}{2} \left[ \left( \phi^2 + \gamma\phi + \Delta\phi^2 + \frac{d\phi}{dt^*} \right) x^2 + \left( c\phi^2 + \gamma\phi + c\Delta\phi^2 + \frac{d\phi}{dt^*} \right) cy^2 \right. \\ \left. + \left( (1+c)\phi^2 - \frac{d\phi}{dt^*} - \gamma\phi + \Delta(1+c)\phi^2 \right) (1+c)z^2 \right], \end{aligned} \quad (10)$$

where  $\gamma = \nu\varepsilon/Ka$  is the first order resistance and  $\Delta = \Gamma\varepsilon^2L/K^{1/2}$  is the second order resistance.

Now we apply the following transformations (Kumari and Nath [6]):

$$\begin{aligned}\eta &= (a/\nu)^{1/2}z, & u &= Uf'(\eta, t^*), & v &= Vs'(\eta, t^*), \\ w &= -(a\nu)^{1/2}\phi(t^*)[f(\eta, t^*) + cs(\eta, t^*)], \\ p_0 - p &= (\rho a^2/2)[(\phi^2 + \gamma\phi + \Delta\phi^2 + d\phi/dt^*)x^2 \\ &\quad + (c\phi^2 + \gamma\phi + c\Delta\phi^2 + d\phi/dt^*)cy^2 + (2\nu/a)P(\eta, t^*)], \\ T - T_\infty &= (T_w - T_\infty)[g_0(\eta, t^*) + (x/L)^2g_1(\eta, t^*) + (y/L)^2g_2(\eta, t^*)] \\ &= (T_w - T_\infty)g(\eta, t^*),\end{aligned}\tag{11}$$

to equations (1)–(5). We get

$$f'''' + \phi(f + cs)f'' + \phi(1 - f'^2) + \phi^{-1}(d\phi/dt^*)(1 - f') + \gamma(1 - f') + \Delta\phi(1 - f'^2) - \partial f'/\partial t^* - \phi^{-1}\chi[g_0 + (x/l)^2g_1 + (y/l)^2g_2] = 0,\tag{12}$$

$$s'''' + \phi(f + cs)s'' + c\phi(1 - s'^2) + \phi^{-1}(d\phi/dt^*)(1 - s') + \gamma(1 - s') + c\phi\Delta(1 - s'^2) - \partial s'/\partial t^* - \phi^{-1}\chi[g_0 + (x/l)^2g_1 + (y/l)^2g_2] = 0,\tag{13}$$

$$\frac{1}{Pr}g_0'' + \phi(f + cs)g_0' - \partial g_0/\partial t^* = 0,\tag{14}$$

$$\frac{1}{Pr}g_1'' + \phi(f + cs)g_1' - 2\phi f'g_1 + E\phi^2 f''^2 - \partial g_1/\partial t^* = 0,\tag{15}$$

$$\frac{1}{Pr}g_2'' + \phi(f + cs)g_2' - 2\phi cs'g_2 + E_1\phi^2 s''^2 - \partial g_2/\partial t^* = 0,\tag{16}$$

$$P = \frac{1}{2}(f + cs)^2\phi^2 + (f' + cs')\phi - \frac{\partial}{\partial t^*} \int_0^\eta (f + cs)\phi\partial\eta.\tag{17}$$

The initial conditions are

$$f = f_i, \quad s = s_i, \quad g_0 = g_{0i}, \quad g_1 = g_{1i}, \quad g_2 = g_{2i} \quad \text{at} \quad t^* = 0,\tag{18}$$

and the boundary conditions are given by

$$\begin{aligned}f = f' = s = s' = 0, \quad g_0 = 1, \quad g_1 = g_2 = 0 &\quad \text{at} \quad \eta = 0, \\ f' \rightarrow 1, \quad s' \rightarrow 1, \quad g_0 = g_1 = g_2 = 0 &\quad \text{as} \quad \eta \rightarrow \infty,\end{aligned}\tag{19}$$

where primes denote the derivative with respect to  $\eta$  and  $E = \frac{\alpha^2 L^2}{c_p(T_w - T_\infty)}$ ,  $E_1 = c^2 E$  are Eckert numbers;  $Pr = \mu c_p/k$  is the Prandtl number.

The corresponding steady-state equations are obtained by putting  $t^* = 0$ ,  $\phi = 1$ ,

$\partial/\partial t^* = 0$  in equations (12)–(16) and they are given by

$$f'''' + (f + cs)f'' + (1 - f'^2) + \gamma(1 - f') + \Delta(1 - f'^2) - \chi[g_0 + (x/l)^2g_1 + (y/l)^2g_2] = 0, \quad (20)$$

$$s'''' + (f + cs)s'' + c(1 - s'^2) + \gamma(1 - s') + c\Delta(1 - f'^2) - \chi[g_0 + (x/l)^2g_1 + (y/l)^2g_2] = 0, \quad (21)$$

$$\frac{1}{Pr}g_0'' + (f + cs)g_0' = 0, \quad (22)$$

$$\frac{1}{Pr}g_1'' + (f + cs)g_1' - 2f'g_1 + Ef'^2 = 0, \quad (23)$$

$$\frac{1}{Pr}g_2'' + (f + cs)g_2' - 2cs'g_2 + E_1s'^2 = 0, \quad (24)$$

$$P = \frac{1}{2}(f + cs)^2 + (f' + cs')\phi, \quad (25)$$

where  $\chi = Gr_x/Re_x^2 = g\beta\Delta T/aU_\infty$  is the mixed convection parameter;  $Gr_x = g\beta(T_w - T_\infty)x^3/\nu^2$  is the local Grashof number,  $Re_x = U_\infty x/\nu$  is the Reynolds number.

The boundary conditions for equations (20)–(24) are given by equations (18), (19).

Here  $\eta$  and  $t^*$  are the transformed independent variables; prime denotes derivative with respect to  $\eta$ ;  $f'$  and  $s'$  are the dimensionless velocity components along  $x$  and  $y$  direction, respectively;  $P$  is the dimensionless pressure;  $L = (\nu/a)^{1/2}$  is the characteristic length;  $a$  and  $b$  are the velocity gradients along  $x$  and  $y$  directions in the potential flow and  $c = b/a$  is their ratio. The function  $\phi(t^*)$  should be chosen such that both  $\phi$  and  $d\phi/dt^*$  are continuous functions.

It may be noted that equations (20) and (21) for  $\gamma = \Delta = \chi = 0$  (clear fluid in forced convection limit) are essentially the same as those of Kumari and Nath [6] but without magnetic field, those of Howarth [13] for the flow in the nodal-point region ( $0 \leq c \leq 1$ ) and those of Davey [14] in the saddle-point region ( $-1 \leq c < 0$ ). Also equation (20) and (22) with  $\gamma = \Delta = \chi = 0$  are identical to those of Kumari and Nath [6] and Hayday and Bowlus [15] in the region ( $0 \leq c \leq 1$ ).

Most the dimensional shapes of practical interest lie between a cylinder ( $c = 0$ ) and a sphere ( $c = 1$ ), which are discussed by Kumari and Nath [6].

The quantities of physical interest are the local skin friction coefficients in  $x$  and  $y$  directions and the local heat transfer coefficient in terms of the Nusselt number.

$$C_{fx} = 2\mu(\partial u/\partial z)_{z=0}/\rho U_\infty^2 = \frac{2}{\sqrt{Re_x}}\phi(t^*)f''(0, t^*), \quad (26)$$

$$C_{fy} = 2\mu(\partial v/\partial z)_{z=0}/\rho U_\infty^2 = \frac{2}{\sqrt{Re_x}}(V_\infty/U_\infty)\phi(t^*)s''(0, t^*), \quad (27)$$

$$\begin{aligned}
Nu_x &= -x(\partial T/\partial z)_{z=0}/(T_w - T_\infty) \\
&= -\frac{1}{\sqrt{Re_x}} [g'_0(0, t^*) + (x/L)^2 g'_1(0, t^*) + (y/L)^2 g'_2(0, t^*)], \\
&= -\frac{1}{\sqrt{Re_x}} g'(0, t^*). \tag{28}
\end{aligned}$$

Where

$$U_\infty = ax, \quad V_\infty = by, \quad Re_x = U_\infty x/\nu, \tag{29}$$

here  $C_{fx}$  and  $C_{fy}$  are the local skin friction coefficients in  $x$  and  $y$  directions, respectively;  $Nu_x$  is the local Nusselt number;  $Re_x$  is the local Reynolds number;  $U_\infty$  and  $V_\infty$  are the components of the velocity in  $x$  and  $y$  direction in the potential flow for the steady-state case. For  $C = 0$ ,  $V_\infty = 0$  and for  $C = 1$ ,  $U_\infty = V_\infty$ .

#### 4 Self-similar equations

The partial differential equations (1)–(5) with four independent variables  $(t, x, y, z)$  can be reduced to a system of ordinary differential equations if the velocity components in  $x$  and  $y$  directions in the potential flow vary directly as a linear function of distance and inversely as a linear function of time. The velocity components are given by

$$U = ax(1 - \lambda t^*)^{-1}, \quad V = by(1 - \lambda t^*)^{-1}, \quad \lambda t^* < 1. \tag{30}$$

From the continuity equation, we get the  $z$ -component of the velocity as

$$w = -a(1 + c)(1 - \lambda t^*)^{-1}z. \tag{31}$$

The wall temperature  $T_{w0}$  is the value of  $T_w$  at  $t^* = 0$  varies

$$T_w - T_\infty = (T_{w0} - T_\infty)(1 - \lambda t^*)^{-2}. \tag{32}$$

From the Bernoulli equation we get the expression for the pressure  $p$  as

$$\begin{aligned}
p_0 - p &= \frac{1}{2}\rho a^2(1 - \lambda t^*)^{-2} [(1 + \lambda + \gamma + \Delta)x^2 + c(c + \lambda + \gamma + c\Delta)y^2] \\
&\quad + (1 + c)[1 + c - \lambda - \gamma + \Delta(1 + c)]z^2. \tag{33}
\end{aligned}$$

We apply the following transformations along with equations (29)–(32)

$$\eta = (a/\nu)(1 - \lambda t^*)^{-1/2}z, \quad t^* = at, \quad u = ax(1 - \lambda t^*)^{-1}f'(\eta), \tag{34}$$

$$v = by(1 - \lambda t^*)^{-1}s'(\eta), \quad w = -(a\nu)(1 - \lambda t^*)^{-1/2}[f(\eta) + cs(\eta)], \tag{35}$$

$$\begin{aligned}
T - T_\infty &= (T_w - T_\infty)[g_0(\eta) + (x/l)^2 g_1(\eta) + (y/l)^2 g_2(\eta)] \\
&= (T_w - T_\infty)g(\eta), \tag{36}
\end{aligned}$$

$$\begin{aligned}
p_0 - p &= \frac{1}{2}\rho a^2(1 - \lambda t^*)^{-2} [(1 + \lambda + \gamma + \Delta)x^2 + c(c + \lambda + \gamma + c\Delta)y^2 \\
&\quad + (2\nu/a)(1 - \lambda t^*p(\eta))] \tag{37}
\end{aligned}$$

to equations (1)–(5) and it is found that (1) is identically satisfied and (2)–(5) reduce to

$$f''' + (f + cs)f'' + (1 - f'^2) + \gamma(1 - f') + \Delta(1 - f'^2) + \lambda(1 - f' - \eta f''/2) - \chi[g_0 + (x/l)^2 g_1 + (y/l)^2 g_2] = 0, \quad (38)$$

$$s''' + (f + cs)s'' + c(1 - s'^2) + \gamma(1 - s') + c\Delta(1 - s'^2) + \lambda(1 - s' - \eta s''/2) - \chi c[g_0 + (x/l)^2 g_1 + (y/l)^2 g_2] = 0, \quad (39)$$

$$\frac{1}{Pr} g_0'' + (f + cs)g_0' - \frac{1}{2}\eta g_0' - 2\lambda g_0 = 0, \quad (40)$$

$$\frac{1}{Pr} g_1'' + (f + cs)g_1' - 2f'g_1 - 2\lambda g_1 - \frac{1}{2}\lambda \eta g_1' + E f''^2 = 0, \quad (41)$$

$$\frac{1}{Pr} g_2'' + (f + cs)g_2' - 2cs'g_2 - 2\lambda g_2 - \frac{1}{2}\lambda \eta g_2' + E_1 s''^2 = 0, \quad (42)$$

$$P = \frac{1}{2}(f + cs)^2 - (\lambda/2)\eta(f + cs). \quad (43)$$

The boundary conditions are given by

$$\begin{aligned} f = f' = s = s' = g_1 = g_2 = 0, \quad g_0 = 1 \quad \text{at} \quad \eta = 0, \\ f' = s' = 1, \quad g_0 = g_1 = g_2 = 0, \quad \text{as} \quad \eta \rightarrow \infty, \end{aligned} \quad (44)$$

here  $\lambda$  is the dimensionless parameter which characterizes the unsteadiness in the flow field. For the accelerating flow  $\lambda > 0$  and for the decelerating flow  $\lambda < 0$ . The above equations reduce to steady-state equations for  $\lambda = 0$  which are given by (20)–(24).

It may be noted that equations (38)–(42) for  $\gamma = \Delta = \lambda = 0$  (clear fluid in forced convection limit) are identical to those of Kumari and Nath [6] without magnetic field. Also equation (28), (39) and (40) with  $\gamma = \Delta = \chi = \lambda = 0$  are the same as those of Teipel [16].

The local skin friction coefficients in  $x$  and  $y$  directions and the local Nusselt number (heat transfer coefficients) are expressed as

$$C_{fx} = 2\mu(\partial u/\partial z)_{z=0}/\rho U^2 = \frac{2}{\sqrt{Re_x}}\phi(t^*)f''(0, t^*), \quad (45)$$

$$C_{fy} = 2\mu(\partial v/\partial z)_{z=0}/\rho U^2 = \frac{2}{\sqrt{Re_x}}(V/U)\phi(t^*)s''(0, t^*), \quad (46)$$

$$\begin{aligned} Nu_x &= -x(\partial T/\partial z)_{z=0}/(T_w - T_\infty) \\ &= -\frac{1}{\sqrt{Re_x}}[g_0'(0, t^*) + (x/L)^2 g_1'(0, t^*) + (y/L)^2 g_2'(0, t^*)], \\ &= -\frac{1}{\sqrt{Re_x}}g'(0, t^*), \end{aligned} \quad (47)$$

where  $Re_x = Ux/\nu$ .

## 5 Method of solution

The partial differential equations governing the semi-similar flow, equations (12)–(16) under boundary conditions (19) and initial conditions (20)–(24), are solved numerically using a finite difference scheme developed by Nakamura [17]. Hence, for the sake of completeness, we present here only an outline of this method. Equations (12)–(16) are coupled non-linear parabolic partial differential equations in  $f, s$  and  $g_i, i = 1, 2, 3$ . First, equations (12) and (13) are linearized and the resulting third-order linear partial differential equations are converted into second order partial differential equations by substituting  $f' = F$  and  $s' = S$ . The variables  $f$  and  $s$  in equations (14), (16) are considered as non-linear coefficients and are evaluated by numerical integration from  $F$  and  $S$ . These linear partial differential equations are discretised using the central difference approximation in the  $\eta$  coordinate and backward difference approximation in the  $t^*$  coordinate. For the time step  $k$ , the discretised equations become tri-diagonal equations. This system of equations for each time step requires an iterative procedure due to the presence of non-linear coefficients. Successive substitution and iteration are continued for each time step until convergence is reached. Equations (20)–(24) under boundary conditions (19) were solved by using a double shooting method in order to accurately obtain the initial values of the various functions at time  $t^* = 0$ .

In a similar manner the systems of equations (38)–(42) with the boundary conditions (44) governing the self-similar flow case also been solved.

## 6 Results and discussion

The partial differential equations (12)–(16) governing the semi-similar flow and the ordinary differential equations (38)–(42) governing the self-similar flow have been solved numerically using the method described earlier. In order to assess the accuracy of the method, we have compared the surface shear stresses in  $x$  and  $y$  directions ( $f''(0), s''(0)$ ) for the steady-state case ( $t^* = 0$ ) when  $\gamma = \Delta = \chi = 0$  (clear fluid in forced convection limit) with those of Kumari and Nath [6], Howarth [13] and Hayday and Bowlus [15] in the nodal point region ( $0 \leq c \leq 1$ ) and with those of Kumari and Nath [6] and Davey [14] in the saddle-point region ( $-1 \leq c < 0$ ). The heat transfer parameter ( $-g'_0(0)$ ) for the nodal-point region when  $E = E_1 = 0$  (without viscous dissipation) are compared with that of Kumari and Nath [6] and Hayday and Bowlus [15]. In all the cases the results are found to be in excellent agreement. The comparison is presented in Tables 1–3.

The variation of the surface shear stresses in  $x$  and  $y$  directions,  $f''(0, t^*), s''(0, t^*)$ , and the surface heat transfer  $-g'(0, t^*)$  with time  $t^*$  for the accelerating flow  $\phi(t^*) = 1 + \delta t^*, \delta = 0.2, c = -0.5, \gamma = 0.0, 0.5, 1.0, \Delta = 0.0, Pr = 0.7, E = E_1 = 0.2, x/l = y/l = 0.2, \chi = 0, 0.5$  is presented in Figs. 2–4. It is observed that as the first resistance parameter  $\gamma$  increases both  $f''(0, t^*)$  and  $s''(0, t^*)$  increases and the magnitude of  $-g'(0, t^*)$ , which characterize the heat transfer rate decreases. However as the mixed convection parameter  $\chi$  increases the surface shear stresses and the surface heat transfer all increase. Also both of  $f''(0, t^*)$  and  $-g'(0, t^*)$  increases with the increase of time  $t^*$

whereas  $s''(0, t^*)$  increases up to certain value of  $t^*$  depends on  $\chi$  and then decreases as  $t^*$  increases.

Table 1. Comparison of surface shear stresses for the steady state case,  $f''(0)$ ,  $s''(0)$ , when  $t^* = 0, 0 \leq c \leq 1$

$c$	Present results		Kumari and Nath [6]		Howarth [13]	
	$f''(0)$	$s''(0)$	$f''(0)$	$s''(0)$	$f''(0)$	$s''(0)$
1.0	1.31194	1.31194	1.3153	1.3153	1.312	1.312
0.75	1.28863	1.16433	1.2892	1.1723	1.288	1.164
0.5	1.26687	0.99813	1.2654	1.0142	1.267	0.998
0.25	1.24761	0.80515	1.2453	0.8378	1.247	0.805
0.0	1.23258	0.57049	1.2268	0.5848	1.233	0.570

Table 2. Comparison of surface shear stresses for the steady state case,  $f''(0)$ ,  $s''(0)$ , when  $t^* = 0, -1 \leq c < 0$

$c$	Present results		Kumari and Nath [6]		Davey [14]	
	$f''(0)$	$s''(0)$	$f''(0)$	$s''(0)$	$f''(0)$	$s''(0)$
-0.1	1.22843	0.45937	1.2282	0.4594	1.2284	0.4594
-0.2	1.22577	0.33533	1.2256	0.3350	1.2258	0.3353
-0.3	1.22501	0.19700	1.2248	0.1973	1.2250	0.1970
-0.4	1.22646	0.04597	1.2262	0.0459	1.2265	0.0460
-0.5	1.23019	-0.11150	1.2304	-0.1113	1.2302	-0.1115
-0.6	1.23593	-0.26659	1.2361	-0.2664	1.2359	-0.2666
-0.7	1.24322	-0.41295	1.2430	-0.4128	1.2432	-0.4130
-0.8	1.25169	-0.54872	1.2519	-0.5485	1.2517	-0.5488
-0.9	1.26115	-0.67521	1.2610	-0.6758	1.2612	-0.6761
-1.0	1.27154	-0.79449	1.2732	-0.8110	1.2729	-0.8112

Table 3. Comparison of surface shear stresses for the steady state case,  $-g'_0(0)$ , when  $t^* = 0, 0 \leq c \leq 1$

$c$	Present results		Kumari and Nath [6]		Hayday and Bowlus [15]	
	$Pr = 0.7$	$Pr = 10$	$Pr = 0.7$	$Pr = 10$	$Pr = 0.7$	$Pr = 10$
1.0	0.66538	1.75208	0.6656	1.7523	0.6654	1.7521
0.75	0.62308	1.64171	0.6233	1.6419	0.6231	1.6417
0.5	0.57967	1.53140	0.5798	1.5311	0.5797	1.5314
0.25	0.53621	1.42634	0.5358	1.4265	0.5362	1.4263
0.0	0.49587	1.33880	0.4957	1.3386	0.4959	1.3389

The variation of the surface shear stresses in  $x$  and  $y$  directions,  $f''(0, t^*)$ ,  $s''(0, t^*)$  and the surface heat transfer  $-g'(0, t^*)$ , with the ratio velocity gradients in the free stream  $c$  (nature of the stagnation point) for  $t^* = 1.5$ ,  $\phi(t^*) = 1 + \delta t^*$ ,  $\delta = 0.2$ ,  $\gamma, \Delta = 0.0, 0.5, 1.0$ ,  $E = E_1 = 0.2$ ,  $Pr = 0.7$ ,  $x/l = y/l = 0.2$ ,  $\chi = 0, 0.5, 1, 3$  are presented in Figs. 5–7. It can be seen from Fig. 5 that the shear stresses in  $x$ -directions,  $f''(0, t^*)$

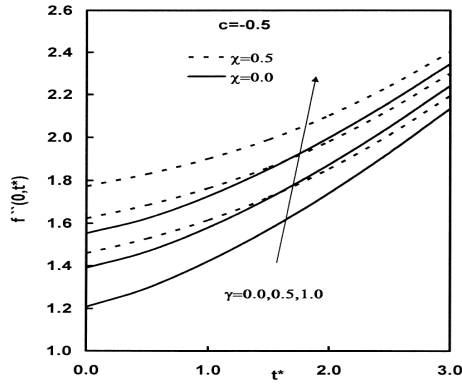


Fig. 2. Variation of the surface shear stress in  $x$ -direction  $f''(0, t^*)$  with time  $t^*$  for the accelerating flow  $\phi(t^*) = 1 + \delta t^{*2}$ ,  $Pr = 0.7$ ,  $\delta = 0.2$ ,  $c = -0.5$ ,  $\Delta = 0.0$  with various values of  $\gamma$  and  $\chi$ .

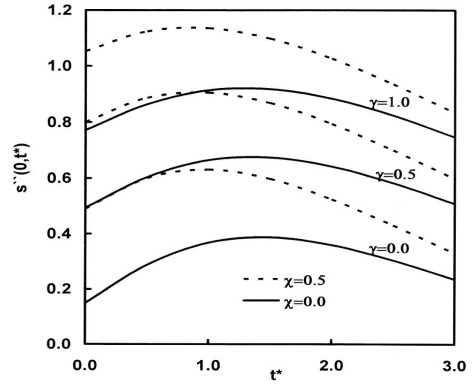


Fig. 3. Variation of the surface shear stress in  $y$ -direction  $s''(0, t^*)$  with time  $t^*$  for the accelerating flow  $\phi(t^*) = 1 + \delta t^{*2}$ ,  $Pr = 0.7$ ,  $\delta = 0.2$ ,  $c = -0.5$ ,  $\Delta = 0.0$  with various values of  $\gamma$  and  $\chi$ .

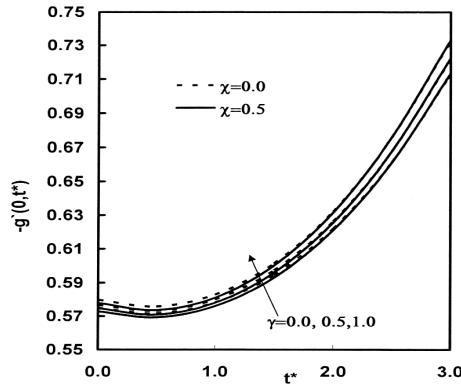


Fig. 4. Variation of the surface heat transfer  $-g'(0, t^*)$  with time  $t^*$  for the accelerating flow  $\phi(t^*) = 1 + \delta t^{*2}$ ,  $Pr = 0.7$ ,  $\delta = 0.2$ ,  $c = -0.5$ ,  $\Delta = 0.0$ ,  $x/L = y/L = 0.1$ ,  $E = E_1 = 0.2$  with various values of  $\gamma$  and  $\chi$ .

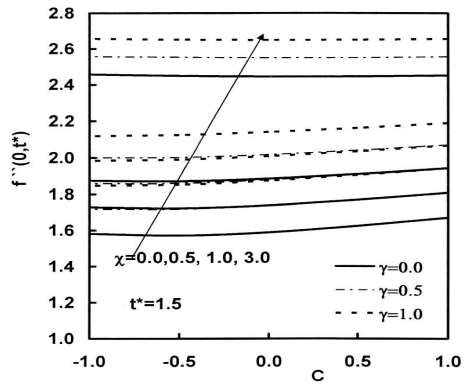


Fig. 5. Variation of the surface shear stress in  $x$ -direction  $f''(0, t^*)$  with  $c$  for the accelerating flow  $\phi(t^*) = 1 + \delta t^{*2}$ ,  $Pr = 0.7$ ,  $\delta = 0.2$ ,  $t^* = 1.5$ ,  $\Delta = 0.0$  with various values of  $\gamma$  and  $\chi$ .

is rather insensitive to the change in  $c$ . This is similar to the forced convection case increase with the first and second order resistances and the mixed convection parameter also increases. Similar trend has been observed by Kumari and Nath [6]. However, the effect of both  $\chi$  and  $\gamma$  parameter is significant. Fig. 6 indicates that the surface shear stresses in  $y$ -directions,  $s''(0, t^*)$ , continuously increases with increasing  $c$  and vanishes at  $c = -0.7536$  for  $\chi = 0$  (forced convection limit) and the reverse flow occurs in the region  $(-1 \leq c < -0.7536)$ . When  $\chi > 0$  there is no reverse flow. Therefore, the increase in the free stream velocity or (and) in the buoyancy force delay or prevent the occurrence of flow reversal. As illustrated in Fig. 7 it is observed that, the surface heat transfer  $-g'(0, t^*)$ , decreases with decreasing  $c, \chi, \gamma$  until at some negative value of  $c$  where the flow is reversed. Consequently, the heat transfer rate increases as  $c, \chi, \gamma$  further increases.

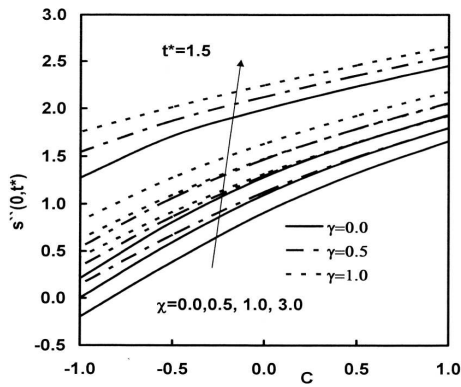


Fig. 6. Variation of the surface shear stress in  $y$ -direction  $s''(0, t^*)$  with  $c$  for the accelerating flow  $\phi(t^*) = 1 + \delta t^{*2}$ ,  $Pr = 0.7$ ,  $\delta = 0.2$ ,  $t^* = 1.5$ ,  $\Delta = 0.0$  with various values of  $\gamma$  and  $\chi$ .

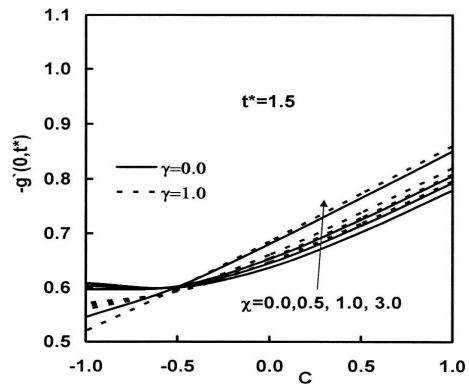


Fig. 7. Variation of the surface heat transfer  $-g'(0, t^*)$  with  $c$  for the accelerating flow  $\phi(t^*) = 1 + \delta t^{*2}$ ,  $Pr = 0.7$ ,  $\delta = 0.2$ ,  $t^* = 1.5$ ,  $c = -0.5$ ,  $\Delta = 0.0$  with various values of  $\gamma$  and  $\chi$ .

The effects of the second order resistance  $\Delta$  on the surface shear stresses in  $x$  and  $y$  directions,  $f''(0, t^*)$ ,  $s''(0, t^*)$  and the surface heat transfer  $-g'(0, t^*)$ , are illustrated in Figs. 8–10. The second order parameter  $\Delta$  has the same trend as the first order parameter  $\gamma$  as discussed in Figs. 5–7.

The velocity profiles  $s'(\eta, t^*)$  for  $\phi(t^*) = 1 + \delta t^{*2}$ ,  $\delta = 0.2$ ,  $t^* = 1.5$ ,  $Pr = 0.7$ ,  $c = -0.5$  with various values of  $\gamma, \Delta$  and  $\chi$  are shown in Fig. 11. It is observed that the magnitude and the region of reverse flow decrease with increasing the mixed convection parameter  $\chi$  and increase with increasing the second order resistance parameter  $\Delta$  while there is no reverse flow for all values of the first order resistance parameter  $\gamma$ . Since the velocity profiles in  $x$ -direction,  $f'(\eta, t^*)$ , and the temperature profiles,  $g(\eta, t^*)$ , show usual features of boundary layer flows [13–15], they are not shown here.

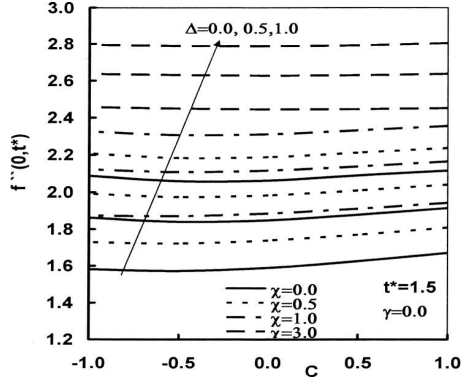


Fig. 8. Variation of the surface shear stress in  $x$ -direction  $f''(0, t^*)$  with  $c$  for the accelerating flow  $\phi(t^*) = 1 + \delta t^{*2}$ ,  $Pr = 0.7$ ,  $\delta = 0.2$ ,  $t^* = 1.5$ ,  $\gamma = 0.0$  with various values of  $\Delta$  and  $\chi$ .

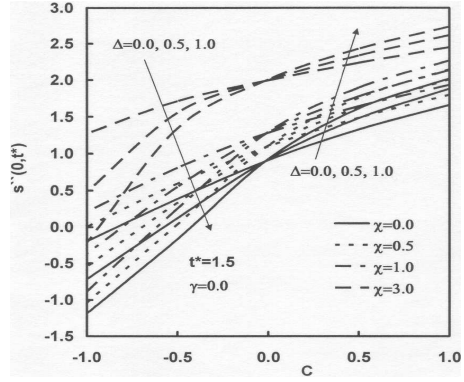


Fig. 9. Variation of the surface shear stress in  $y$ -direction  $s''(0, t^*)$  with  $c$  for the accelerating flow  $\phi(t^*) = 1 + \delta t^{*2}$ ,  $Pr = 0.7$ ,  $\delta = 0.2$ ,  $t^* = 1.5$ ,  $\gamma = 0.0$  with various values of  $\Delta$  and  $\chi$ .

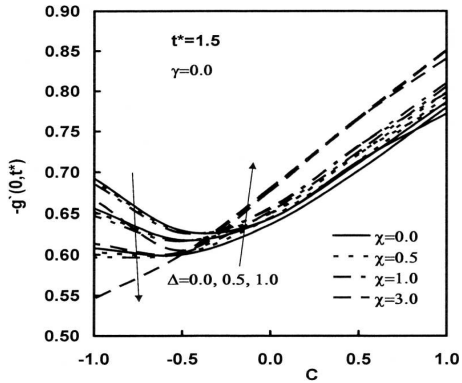


Fig. 10. Variation of the surface heat transfer  $-g'(0, t^*)$  with  $c$  for the accelerating flow  $\phi(t^*) = 1 + \delta t^{*2}$ ,  $Pr = 0.7$ ,  $\delta = 0.2$ ,  $t^* = 1.5$ ,  $\gamma = 0.0$  with various values of  $\Delta$  and  $\chi$ .

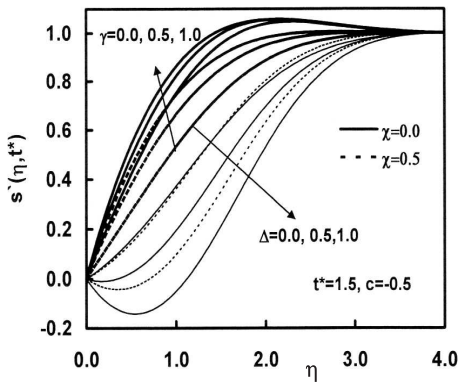


Fig. 11. Effect of the first and second resistance parameters  $\gamma$  and  $\Delta$  on the velocity profiles in  $y$ -direction,  $s'(\eta, t^*)$ , with  $\phi(t^*) = 1 + \delta t^{*2}$ ,  $Pr = 0.7$ ,  $\delta = 0.2$ ,  $t^* = 1.5$ ,  $c = -0.5$  and  $\chi = 0.0, 0.5$ .

## 7 Conclusions

Equations of motion and energy governing the unsteady mixed convection flow of a viscous fluid in near a stagnation point of a general three-dimensional body embedded in a porous media are integrated. The velocity in the potential flow is assumed to vary arbitrary with time. The non-Darcy effects including convective, boundary and inertial effects are included in the analysis. Both nodal-point region and saddle-point region are considered. The semi-similar solutions of the momentum and energy equations are obtained

numerically using finite difference method. Also a self-similar solution is found when the velocity in the potential flow and the wall temperature vary with time in particular manner. Many results are obtained and a representative set is displayed graphically to illustrate the influence of the physical parameters on the surface shear stresses and the surface heat transfer. Whenever possible, these results are compared with available numerical solutions and found to be highly accurate. The results indicate that significant changes occur in the shear stresses and the surface heat transfer. For a certain negative value of the parameter  $c$ , flow reversal takes place in the velocity component in  $y$ -direction. The buoyancy force or (and) the accelerating free stream velocity tends to delay or prevent flow reversal. The presence of the buoyancy force and the solid matrix increases the shear stress in  $x$  and  $y$  directions and the surface heat transfer.

## References

1. C. H. Johnson, P. Cheng, Possible similarity solutions for free convection boundary layers adjacent to flat plates in porous media, *Int. J. Heat Mass Transfer*, **21**, pp. 709–718, 1978.
2. R. Bradean, P. J. Heggs, D. B. Ingham, I. Pop, Convective heat flow from suddenly heated surfaces embedded in porous media, in: *Transport Phenomena in Porous Media*, D. B. Ingham, I. Pop (Eds.), Pergamon, Oxford, pp. 411–438, 1998.
3. I. Pop, D. B. Ingham, *Convective Heat Transfer: Mathematical and Computational Modeling of Viscous Fluids and Porous Media*, Pergamon, Oxford, 2001.
4. X. Hang, S. J. Liao, I. Pop, Series solutions of unsteady free convection flow in the stagnation-point region of a three-dimensional body, *International Journal of Thermal Sciences*, (in press, corrected proof, available online 15 June 2007).
5. A. T. Eswara, G. Nath, Effect of large injection rates on unsteady mixed convection flow at a three-dimensional stagnation point, *International Journal of Non-Linear Mechanics*, **34**, pp. 85–103, 1999.
6. M. Kumari, G. Nath, Unsteady flow and heat transfer of a viscous fluid in the stagnation region of a three-dimensional body with a magnetic field, *Int. J. Eng. Sci.*, **40**, pp. 411–432, 2002.
7. R. Nazar, N. Amin, I. Pop, Unsteady mixed convection boundary layer flow near the stagnation point on a vertical surface in a porous medium, *Int. J. Heat Mass Transfer*, **47**, pp. 2681–2688, 2004.
8. J. H. Merkina, I. Pop, Free convection near a stagnation point in a porous medium resulting from an oscillatory wall temperature, *Int. J. Heat Mass Transfer*, **43**, pp. 611–621, 2000.
9. I. A. Hassanien, F. S. Ibrahim, Gh. M. Omer, Unsteady flow and heat transfer of a viscous fluid in the stagnation region of a three-dimensional body embedded in a porous medium, *J. Porous Media*, **9**, pp. 357–372, 2006.
10. S. Shafie, N. Amin, I. Pop, g-Jitter free convection flow in the stagnation-point region of a three-dimensional body, *Mechanics Research Communications*, **34**, pp. 115–122, 2007.
11. F. C. Lai, Mixed convection in saturated porous media, in: *Handbook of Porous Media*, K. Vafai (Ed.), Marcel Dekker, pp. 605–661, New York, 2000.

12. W. H. H. Banks, Three-dimensional free convection near a two-dimensional isothermal surface, *J. Eng. Math.*, **6**, pp. 109–115, 1972.
13. L. Howarth, Philos. The boundary layer on three-dimensional flow, Part 2, *Magazine*, **42**, p. 1433, 1951.
14. A. Davey, Boundary-layer flow at a saddle point of attachment, *J. Fluid Mech.*, **10**, pp. 593–610, 1961.
15. A. A. Hayday, D. A. Bowlus, Integration of coupled nonlinear equations in boundary-layer theory with specific reference to heat transfer near the stagnation point in three-dimensional flow, *Int. J. Heat Mass Transfer*, **10**, pp. 415–426, 1967.
16. I. Teipel, Heat transfer in unsteady laminar boundary layers at an incompressible three-dimensional stagnation flow, *Mech. Res. Comm.*, **6**, pp. 27–32, 1979.
17. S. Nakamura, Iterative finite-difference schemes for similar and nonsimilar boundary layer equations, *Advances in Engineering Software*, **21**, pp. 123–131, 1994.